計算数理工学論文集 Vol. 4 (2004 年 7 月), 論文 No. 04-070918 JASCOME

Boundary element method for nonlinear thermoelasticity with temperature dependent material properties

Toshiro MATSUMOTO[1], Artur GUZIK[2†] and Masataka TANAKA[3]

1) Nagoya University, Furo-cho, Chikusa-ku, Nagoya 464-8603, (E-mail: t.matsumoto@nuem.nagoya-u.ac.jp)
2) Shinshu University, 4-17-1 Wakasato, Nagano 380-8553, (E-mail: guzik@homer.shinshu-u.ac.jp)
3) Shinshu University, 4-17-1 Wakasato, Nagano 380-8553, (E-mail: dtanaka@gipwc.shinshu-u.ac.jp)
† while on leave from Cracow University of Technology, Cracow, Poland

In this paper, the DR-BEM formulation for analysis of thermoelasticity problems is presented. The derived particular solutions for displacements and tractions are provided and, moreover, numerical implementation is briefly discussed. The method ensures a meshless treatment of domain integrals and numerically efficient algorithm for analysis of thermoelastic deformations in an arbitrary geometry and loading conditions. The validity and the high accuracy of the formulation are demonstrated considering a series of examples, in which obtained calculation results are compared with analytical and/or FEM solutions.

Key Words: Thermoelasticity, Boundary Element Method, Dual Reciprocity Method

1. Introduction

One of the most crucial and time-consuming parts of any numerical simulation is the discretization of the domain of interest. An implementation of the *Boundary Element Method* (BEM) as a numerical technique not only simplifies this task, as only surface mesh is generated, but also provides highly accurate calculation results for all variables of interest, which in thermoelasticity problems are: displacements, strains, and stresses. However, the integral representation of the governing differential equation for thermoelastic deformation contains, originated from the thermal strain, a domain integral term. In the case of *constant isotropic* material properties this integral can be effectively converted to an equivalent boundary one by techniques which use the Galerkin tensors, particular solutions or *Radial Integration Method*[(1)]. Unfortunately, in many engineering applications material properties exhibit dependency on temperature, and these techniques fail for such a nonlinear problem. Present BEM procedures for non-linear thermoelasticity involve, in this situation, discretization of the domain of interest into internal cells. Naturally, it is highly undesirable approach, as one of the main advantages of the BEM, namely boundary-only discretization, is lost.

The *Dual Reciprocity Method* (DRM)[(2)] is a robust technique, which can deal with domain integrals originated from an arbitrary in-homogeneous term of the governing differential equation. In this method, the body force quantities are approximated by a series of prescribed basis functions, and then transformed to the boundary integrals employing particular solutions.

This paper presents a general, DRM-based BEM formulation for thermoelasticity problems, capable of handling nonlinear material properties, arbitrary geometry and loading conditions, providing meshless treatment of domain integrals.

The next Section presents the boundary integral formulation for steady-state thermoelasticity, while in the following Sections the derived particular solutions are outlined, and numerical implementation of the technique is briefly discussed. Finally, a series of examples, validating the derived formulation and demonstrating its high accuracy, is presented.

2. BIE formulation for thermoelasticity

Mathematical model of general isotropic steady-state thermoelasticity contains:

- equilibrium equation

$$\sigma_{ij,i} + B_j = 0 \tag{1}$$

- constitutive equation

$$\sigma_{ij} = \lambda \delta_{ij} \varepsilon_{kk} + 2\mu \varepsilon_{ij} - D\psi \delta_{ij} \tag{2}$$

- and (linear) strain-displacement relationship

$$\varepsilon_{ij} = \frac{1}{2}\left(u_{i,j} + u_{j,i}\right) \tag{3}$$

where

$$D = 3\lambda + 2\mu \tag{4}$$

$$\psi = \int_{\theta_{ref}}^{\theta} \alpha\left(\theta\right) d\theta \tag{5}$$

In the foregoing equations σ, ε, u, and θ stand for stress, (total) strain, displacement, and temperature, respectively, while α, δ_{ij}, λ, μ, and θ_{ref} denote coefficient of thermal expansion, Kronecker's symbol, Lamé's constants, and reference (stress-free) temperature. In this study, it is assumed that both modulus of elasticity, E, and coefficient of thermal expansion, α, are known functions of temperature, while Poisson's ratio, ν, is temperature invariant.

Substituting the constitutive relation into the equilibrium equation and neglecting the mechanical body forces, B_j, yields Navier's (governing) equation:

$$\left(\lambda + \mu\right) u_{i,ji} + \mu u_{j,ii} + \mu_{,i}\left(u_{i,j} + u_{j,i}\right) + \lambda_{,j}\, u_{i,i} - D\psi_{,j} - D_{,j}\psi = 0 \tag{6}$$

Exploiting the definitions of Lamé's constants and normalizing Eq. (6) by value of modulus of elasticity, $E\left(\theta\right)$, gives:

$$\bar{\mu}\, u_{j,ii} + (\bar{\lambda} + \bar{\mu}) u_{i,ji} + \bar{b}_j = 0 \tag{7}$$

where

$$\bar{b}_j = -\frac{1}{E\left(\theta\right)}[\bar{\mu} E_{,i}\left(\theta\right)\left(u_{i,j} + u_{j,i}\right) + \bar{\lambda} E_{,j}\left(\theta\right) u_{i,i} - \bar{D} E_{,j}\left(\theta\right)\psi - \bar{D} E\left(\theta\right)\psi_{,j}] \tag{8}$$

and

$$\bar{\lambda} = \frac{\nu}{\left(1 - 2\nu\right)\left(1 + \nu\right)} \tag{9}$$

$$\bar{\mu} = \bar{G} = \frac{1}{2\left(1 + \nu\right)} \tag{10}$$

$$\bar{D} = 3\bar{\lambda} + 2\bar{\mu} \tag{11}$$

The derivatives of modulus of elasticity and thermal expansion, appearing in (8), can be re-expressed using the chain rule as:

$$E_{,j}\left(\theta\right) = E_{,\theta}\theta_{,j} \tag{12}$$

$$\psi_{,j}\left(\theta\right) = \psi_{,\theta}\theta_{,j} \tag{13}$$

and, thus, Eq. (8) restated in the form of:

$$\bar{b}_j = b_1 + b_2 + b_3 + b_4 \tag{14}$$

where

$$b_1 = -\bar{\mu}\frac{E_{,\theta}}{E}\theta_{,i}\left(u_{i,j} + u_{j,i}\right) \tag{15}$$

$$b_2 = -\bar{\lambda}\frac{E_{,\theta}}{E}\theta_{,j} u_{i,i} \tag{16}$$

$$b_3 = \bar{D}\psi\frac{E_{,\theta}}{E}\theta_{,j} \tag{17}$$

$$b_4 = \bar{D}\alpha\theta_{,j} \tag{18}$$

Integral representation of Navier's Eq. (6) is obtained by employing fundamental solutions and integrating by parts to give:

$$c_{jm} u_j + \int_\Gamma \left(t^*_{jm} u_j - u^*_{jm} t_j\right) d\Gamma - \bar{D}\int_\Gamma t^*_{jm}\psi n_j\, d\Gamma = -\int_\Omega u^*_{jm} b_j\, d\Omega \tag{19}$$

where u^*_{jm} and t^*_{jm} denote fundamental solutions for displacements and tractions, respectively, and Ω and Γ stand for domain and its boundary. The domain integral (on the right-hand side) of (19) is converted to the boundary one by means of the *Dual Reciprocity Method*[2] (DRM). The in-homogeneous term is approximated by means of:

$$b_j = \sum_{l=1}^{N+L} \beta^l_j f(x, z^l) \tag{20}$$

where β^l_j, $f(x, z^l)$, N, and L are approximation coefficients, approximating (basis) functions, numbers of boundary and internal DRM collocation points, respectively. Substituting it into original differential equation, multiplying by the fundamental solution and integrating by parts yields the final form of integral representation given by:

$$c_{jm} u_j + \int_\Gamma t^*_{jm} u_j\, d\Gamma - \int_\Gamma u^*_{jm} t_j\, d\Gamma - \bar{D}\int_\Gamma t^*_{jm}\psi n_j\, d\Gamma = \sum_{l=1}^{N+L} \beta^l_j \left\{ c_{jm}\hat{u}_{jn} + \int_\Gamma t^*_{jm}\hat{u}_{jn}\, d\Gamma - \int_\Gamma u^*_{jm}\hat{t}_{jn}\, d\Gamma \right\} \tag{21}$$

where $\hat{u}_{jn}$ and $\hat{t}_{jn}$ are particular solutions, which are derived and briefly discussed in the next Section.

3. Particular solutions

In this paper, particular solutions of Navier's equation:

$$\bar{\lambda}\hat{u}_{kn,jk} + \bar{\mu}\left(\delta_{ik}\delta_{jl} + \delta_{il}\delta_{jk}\right)\hat{u}_{kn,li} = \delta_{l\,n} f(x, z^l) \tag{22}$$

are obtained by means of *Hörmander method*,[3] namely:

$$\hat{u} = L^c \phi \tag{23}$$

where:

$$\phi = \frac{f}{\det L} \tag{24}$$

and L is the differential operator, L^c its co-factors, while f is a vector of known terms (an approximation functions here). For the problems under consideration it leads to:

$$\hat{u}_{ij} = (\bar{\lambda} + 2\bar{\mu})\nabla^2\Phi\,\delta_{ij} - (\bar{\lambda} + \bar{\mu})\Phi_{,ij} \tag{25}$$

and

$$\hat{t}_{ij} = A\left[\frac{2\nu}{1-2\nu}r_{,j}n_i + r_{,i}n_j + \delta_{ij}r_{,k}n_k\right] - B\left[\frac{2\nu}{1-2\nu}r_{,j}n_i + 2r_{,j}r_{,i}r_{,k}n_k\right] - C\left[\frac{2\nu(\delta_{kk}-1)+2}{1-2\nu}r_{,j}n_i + r_{,i}n_j + \delta_{ij}r_{,k}n_k\right] \quad (26)$$

Assuming that the approximating functions are of radial basis[4], coefficients A, B, and C are calculated from:

$$A = \frac{1}{2(1-\nu)}\left[2(1-v)\frac{d\bar{\Phi}_{,kk}}{dr} - \frac{d}{dr}\left(\frac{1}{r}\frac{d\bar{\Phi}}{dr}\right)\right] \quad (27)$$

$$B = \frac{1}{2(1-\nu)}\left[\frac{d}{dr}(P) - \frac{2}{r}(P)\right] \quad (28)$$

$$C = \frac{1}{2(1-\nu)}\frac{1}{r}P \quad (29)$$

$$P = \frac{d^2\bar{\Phi}}{dr^2} - \frac{1}{r}\frac{d\bar{\Phi}}{dr} \quad (30)$$

where r stands for the Euclidean distance. The table 1 lists expressions for Φ and $\bar{\phi}$, which form depends on the dimensionality of considered problem.

Table 1 Definitions of terms Φ and $\bar{\phi}$

term	2D	3D
$\det L$	$\bar{\mu}(\bar{\lambda}+2\bar{\mu})\nabla^4$	$\bar{\mu}^2(\bar{\lambda}+2\bar{\mu})\nabla^6$
$\bar{\phi}$	$\bar{\mu}(\bar{\lambda}+2\bar{\mu})\phi$	$\bar{\mu}^2(\bar{\lambda}+2\bar{\mu})\phi$
Φ	$\phi_{,kk}$	$\bar{\mu}\phi_{,kkll}$

Once the expression for approximating function f is set, particular solutions from (25) and (26) are determined. In this study, as approximation functions the *Compactly Supported Radial Basis Functions* (CS-RBF) (Wendland's [5] functions) are employed[6][7].

4. Numerical implementation

The process of standard BEM discretization of (21) leads to the set of algebraic equations in the form of:

$$[\mathbf{H}]\{\mathbf{u}\} - [\mathbf{G}]\{\mathbf{t}\} = \left[[\mathbf{H}][\hat{\mathbf{u}}] - [\mathbf{G}][\hat{\mathbf{t}}]\right][\mathbf{F}]^{-1}\{\mathbf{b}\} + [\mathbf{G}]\{\boldsymbol{\Psi}\} \quad (31)$$

where $[\mathbf{H}]$, $[\mathbf{G}]$, $\{\mathbf{u}\}$, $\{\mathbf{t}\}$, $[\hat{\mathbf{u}}]$, $[\hat{\mathbf{t}}]$ stand for coefficient matrices, vectors of displacements and tractions and their particular solutions, respectively, and where thermal expansion is defined as:

$$\{\boldsymbol{\Psi}\} = \bar{D}\psi\{\mathbf{n}\} \quad (32)$$

where $\{\mathbf{n}\}$ denotes the outward normal vector. Calculation of the entries of vector $\{\mathbf{b}\}$ involves obtaining the derivatives of temperature and displacements with respect to coordinates. In this study, these derivatives are evaluated by means of approximating functions, $f(x, z^l)$, as presented in [8], namely:

$$\theta_{,i} = \mathrm{diag}\left\{[\mathbf{F}]_{x_i}[\mathbf{F}]^{-1}\{\theta\}\right\} \quad (33)$$

$$\mathbf{u}_{i,j} = [\mathbf{F}]_{x_j}[\mathbf{F}]^{-1}\{\mathbf{u}\}_i \quad (34)$$

where $[\mathbf{F}]$ and $[\mathbf{F}]_{x_i}$ denote the matrices of approximation functions and their derrivatives, respectively. Hence, entries to $\{\mathbf{b}\}$ can be expressed as:

$$\{\mathbf{b}\} = \{\mathbf{b}\}_1 + \{\mathbf{b}\}_2 + \{\mathbf{b}\}_3 + \{\mathbf{b}\}_4 \quad (35)$$

where

$$\{\mathbf{b}\}_1 = \bar{\mu}[\varphi]_i\left[[\mathbf{F}]_{x_i}[\mathbf{F}]^{-1}\{\mathbf{u}\}_j + [\mathbf{F}]_{x_j}[\mathbf{F}]^{-1}\{\mathbf{u}\}_i\right] \quad (36)$$

$$\{\mathbf{b}\}_2 = \bar{\lambda}[\varphi]_i[\mathbf{F}]_{x_i}[\mathbf{F}]^{-1}\{\mathbf{u}\}_i \quad (37)$$

$$\{\mathbf{b}\}_3 = -\bar{D}[\varphi]_j\{\boldsymbol{\Psi}\} \quad (38)$$

$$\{\mathbf{b}\}_4 = -\bar{D}\,\mathrm{diag}\{\alpha\}[\mathbf{F}]_{x_j}[\mathbf{F}]^{-1}\{\theta\} \quad (39)$$

with

$$[\varphi]_i = \mathrm{diag}\left\{\mathrm{diag}\{\mathbf{S}\}[\mathbf{F}]_{x_i}[\mathbf{F}]^{-1}\{\theta\}\right\} \quad (40)$$

$$S_i = \frac{1}{E}E_{,\theta} \quad (41)$$

Right-hand side of Eq. (31) is temperature dependent, however, as the temperature is known/obtained by thermal analysis, the set is solved in one step. It is worth noting that the presented implementation involves many symmetric, anti-symmetric, and diagonal matrices, what can be exploited to the full extent while coding and solving. Furthermore, the DRM related matrices are calculated only once, as their values dependent on geometry/location, only. Usually, thermal problem is solved prior to structural analysis and those matrices are already generated and can be readily re-used. All that results in an effective numerical implementation, capable of handling non-linear material properties, arbitrary geometry and loading conditions, providing meshless treatment of domain integrals and highly accurate calculation results. This is presented in the next Section.

5. Validation examples

This Section includes a series of benchmark tests, validating the derived formulation. The first example deals with linear thermoelasticity while in the second the fully nonlinear analysis is performed. In all tests presented here, the RBF of class C^2 are used, namely:

$$f(r) = (1-\bar{r})^4(4\bar{r}+1) \quad (42)$$

where $\bar{r}$ stands for normalized radius. The selected class of RBF ensures stability of calculation results. The higher orders of basis function (higher RBF classes, *i.e.* C^6) have a higher convergence rate but may lead to computational

instability. The calculation results are compared with analytical and/or FEM solutions. Analytical solutions were derived (by the authors) for 1D cases. In order to compare their solution results with 3D BEM models, an appropriate boundary conditions (of roller type), to produce the unidirectional deformations, are imposed.

5.1. Example 1 - linear analysis

The geometry of the domain and its dimensions, generated BEM mesh, and location of DRM points are given in Figs. 1, 2, and 3, respectively. The domain surfaces are discretized with 192 (quadratic) boundary elements and, to enhance interpolation of the domain terms, 200 internal nodes are employed.

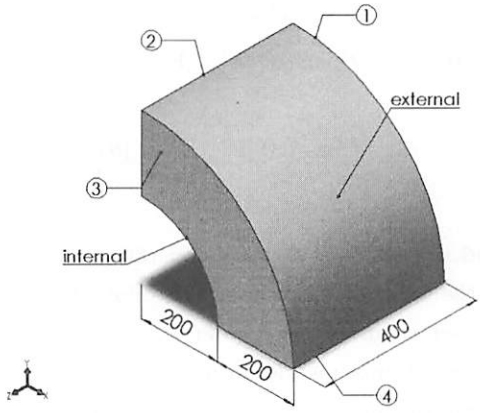

Fig. 1 Domain geometry and dimensions.

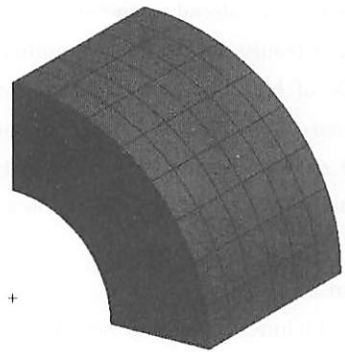

Fig. 2 BEM surface mesh.

For material properties, the following values are assumed: $E = 10^4$ [Pa], $\nu = 0.3$, $\alpha = 1.0 \times 10^{-5}$ [1/K]. Constant material properties allow us to validate and assess the accuracy of terms $\{\mathbf{b}\}_3$ and $\{\mathbf{b}\}_4$ in Eq. (35), as all other terms on the right-hand-side of it vanish. In order to produce the unidirectional deformation, the roller type boundary conditions are applied at surfaces 1-4.

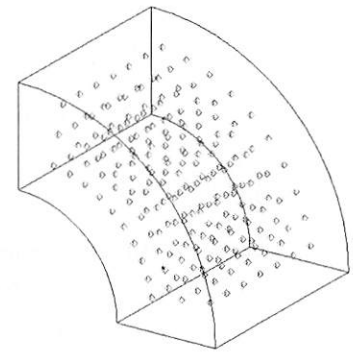

Fig. 3 Location of DRM points.

The following load cases are considered:

- **case A** - uniform temperature: $\Delta\theta = \theta - \theta_{ref} = 100$ [°C]
- **case B** - surface temperatures: $\theta_1 = 200$ [°C] (internal), $\theta_2 = 20$ [°C] (external), reference: $\theta_{ref} = 0$ [°C]
- **case C** - surface temperatures: $\theta_1 = 200$ [°C] (internal), $\theta_2 = 20$ [°C] (external), reference: $\theta_{ref} = 50$ [°C], pressure: $p_1 = 8$ [Pa] (internal)

Fig. 4 presents selected calculation results, demonstrating their high accuracy for all considered load cases.

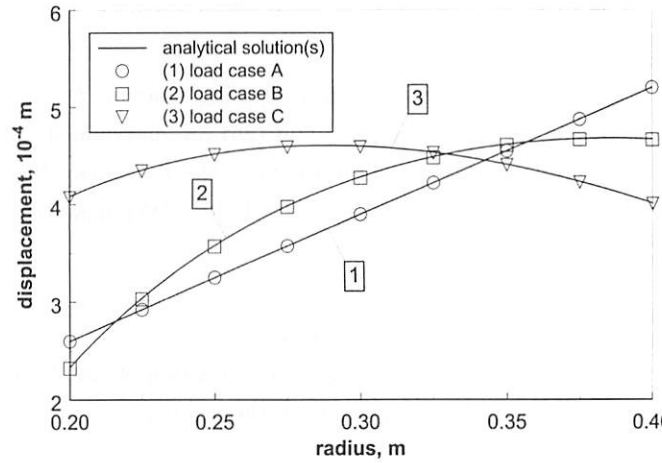

Fig. 4 Calculation results (example 1).

5.2. Example 2 - non-linear problem

In this example two sub-problems are considered. The first deals with the non-linear structural analysis (with prescribed temperature distribution) and obtained results are compared with analytical solution. The second test considers the nonlinear thermal and structural problems. In the latter the BEM and FEM solutions are compared.

5.2.1. Non-linear structural problem The domain,

its dimensions and BEM mesh are those of the foregoing example (Figs. 1, 2, and 3). The material properties, namely, modulus of elasticity and coefficient of thermal expansion, are given by:

$$E = E_0 \exp(E_1 \theta) \tag{43}$$

$$\alpha = \alpha_0 + \alpha_1 \theta \tag{44}$$

where:

- **(material 1)** $E_0 = 140$ [GPa], $E_1 = 0.0033$ [1/°C] and $\alpha_0 = 19.45 \cdot 10^{-6}$ [1/°C], $\alpha_1 = -5.90 \cdot 10^{-9}$ $\left[1/°C^2\right]$, $\nu = 0.3$
- **(material 2)** $E_0 = 450$ [GPa], $E_1 = -0.002$ [1/°C] and $\alpha_0 = 16.80 \cdot 10^{-6}$ [1/°C], $\alpha_1 = 3.00 \cdot 10^{-9}$ $\left[1/°C^2\right]$, $\nu = 0.33$

The variation of material properties with temperature is shown in Fig. 5.

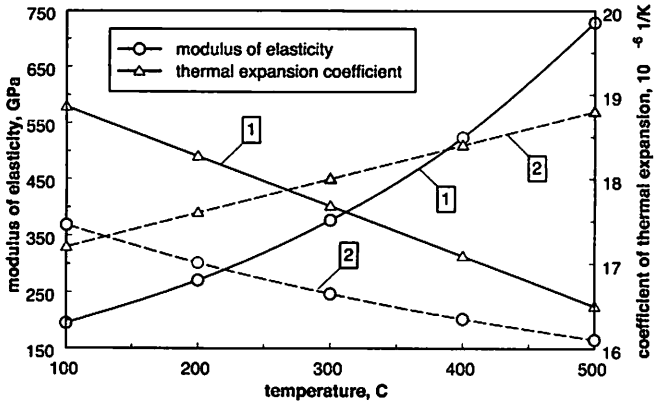

Fig. 5 Material properties (example 2).

As known temperature distribution, the following function is assumed:

$$\theta = \theta_2 + (\theta_1 - \theta_2) \frac{\ln(R_2/r)}{\ln(R_2/R_1)} \tag{45}$$

where R_1 and R_2 are an internal and external radii, respectively (Fig. 1). The data set in this example allows us to validate terms $\{\mathbf{b}\}_1$ and $\{\mathbf{b}\}_2$ in Eq. (35). The following load cases are considered:

for **material 1**:

- **case A** - surface temperatures: $\theta_1 = 350$ [°C] (internal), $\theta_2 = 100$ [°C] (external), reference: $\theta_{ref} = 100$ [°C], pressures: $p_1 = 4$ [MPa] (internal), $p_2 = 1$ [MPa] (external)
- **case B** - surface temperatures: $\theta_1 = 400$ [°C] (internal), $\theta_2 = 150$ [°C] (external), reference: $\theta_{ref} = 200$ [°C], pressures: $p_1 = p_2 = 0$;

and for **material 2**:

- **case C** - surface temperatures: $\theta_1 = 500$ [°C] (internal), $\theta_2 = 100$ [°C] (external), reference: $\theta_{ref} = 140$ [°C], pressures: $p_1 = 3$ [MPa] (internal), $p_2 = 0$ (external)

The BEM calculation results are compared with analytical solution and presented in Fig. 6. Again, in all considered cases high accuracy is achieved.

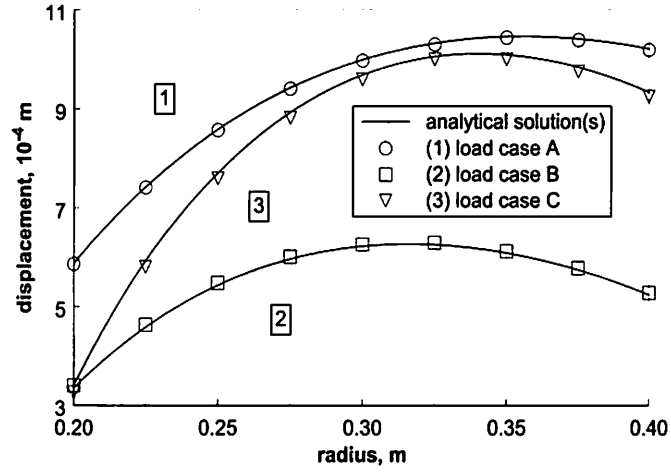

Fig. 6 Results (example 2).

5.2.2. Nonlinear thermal and structural problems In this example, the nonlinear thermal and structural models are considered and results obtained by means of the BEM and FEM compared. The BEM solution of thermal problem is obtained by employing procedure presented in[9]. That technique is also based on DRM and, as mentioned in Section 4, allows us to reuse interpolation matrices, making the presented approach numerically efficient.

The domain geometry and (surface) BEM mesh are kept of previous examples, while (domain) FEM mesh comprises quadratic hexahedral elements. Mesh details are listed in Table 2.

Table 2 Mesh details (example 3)

model	elements	nodes		type
		boundary	internal	
FEM	192	627	490	H20
BEM	208	627	209	Q8

As boundary conditions the following values are applied: surface temperatures: $\theta_1 = 300$ [°C] (internal), $\theta_2 = 100$ [°C] (external), pressures: $p_1 = 4$ [MPa] (internal), $p_2 = 1$ [MPa] (external), $\theta_{ref} = 0$ [°C]. To ensure the generated FEM and BEM models are equivalent, the material properties are

assumed as a linear functions of temperature, namely:

$$E = 217.50 - 0.075\,\theta \quad [\text{GPa}] \tag{46}$$

$$\alpha = 2.2 \times 10^{-5} + 6.4 \times 10^{-9}\theta \quad [1/^\circ\text{C}] \tag{47}$$

$$k = 98.43 - 0.09155\,\theta \quad [\text{W}/(\text{m}^\circ\text{C})] \tag{48}$$

where k is the thermal conductivity. In many commercial FEM packages the program internally evaluates the function at discrete temperature points with linear interpolation between those points, that is, piece-wise linear representation is actually used, *i.e.*[10]. Table 3 lists calculations results. The temperature distribution obtained by means of FEM and BEM is, additionally, compared with analytical solution (which is readily available for thermal problem).

Table 3 Comparison of calculation results (example 3). Units: [m] and [°C]

parameter	analytical	BEM	FEM
$\theta\,(r = 0.25)$	230.43	230.42	230.50
$\theta\,(r = 0.30)$	177.58	177.58	177.63
$\theta\,(r = 0.35)$	135.21	135.21	135.24
$u\,(r = 0.20)$	–	0.00101	0.00104
$u\,(r = 0.25)$	–	0.00144	0.00148
$u\,(r = 0.35)$	–	0.00191	0.00197
$u\,(r = 0.40)$	–	0.00204	0.00209

The small differences in values of displacements are a consequence of differences in results obtained in thermal analysis (FEM analysis gives higher values of temperature comparing to BEM and analytical solution). As material properties (in all examples presented in this paper) vary highly with temperature, it naturally influences results of subsequent structural analysis.

6. Conclusions

In this paper, the general DR-BEM formulation for analysis of non-linear thermoelasticity problems was presented. The required particular solutions for displacements and tractions were derived and provided. Furthermore, numerical implementation was outlined and its features were briefly discussed. The method ensures the meshless treatment of domain integrals and numerically efficient algorithm for analysis of thermoelastic deformations in an arbitrary geometry, under arbitrary loading conditions, and capable of handling materials with temperature dependent properties. The validity and the high accuracy of the formulation were demonstrated considering a series of numerical examples, in which all obtained results were compared with analytical and/or FEM solutions.

Acknowledgments This research was partially supported by *Japan Society for Promotion of Science* (AG & MT) and the *Ministry of Education, Science, Sports and Culture*, Grant-in-Aid for Scientific Research (C), No.15560068, 2003 (TM). The support is gratefully acknowledged.

References

(1) Gao, X.W., Boundary element analysis in thermoelasticity with and without internal cells, *Int. J. Numer. Meth. Engng*, **57** (2003), pp. 975–990.

(2) Partridge P.W., Brebbia C.A., Wrobel L.C., *The Dual Reciprocity Boundary Element Method*, Computational Mechanics Publications, (1992).

(3) Hörmander, L., *Linear partial differential operators*, Springer-Verlag, Berlin, (1969).

(4) Partridge, P.W., Towards criteria for selecting approximation function in the dual reciprocity method, *Engineering Analysis with Boundary Elements*, **24** (2000), pp. 519–529.

(5) Wendland, H., Piecewise polynomial, positive definite and compactly supported radial functions of minimal degree, *Adv. Comput. Math.*, **4** (1995), pp. 389–396.

(6) Chen, C.S., Brebbia C.A. and Power, H., Dual reciprocity method using compactly supported radial basis functions, *Commun. Numer. Meth. Engng.*, **15** (1999), pp. 137–150.

(7) Golberg, M.A., Chen, C.S. and Bowman, H., Some recent results and proposals for the use of radial basis functions in the BEM, *Engineering Analysis with Boundary Elements*, **23** (1999), pp. 285–296.

(8) Tanaka, Masa., Matsumoto, T. and Suda, Y., A dual reciprocity boundary element method applied to the steady-state heat conduction problem of functionally gradient materials, *Electronic Journal of Boundary Elements*, Vol.BETEQ 2001, No.1, (2002), pp. 128–135.

(9) Tanaka, Masa., Matsumoto, T. and Takakuwa, S., DRM applied to the time-stepping BEM for transient heat conduction, Gallego, R, Alliabadi, MH (eds.) *Proceedings BeTeQ Conference*, (2003), Granada, Spain, pp. 79–84.

(10) *ANSYS 7.1 Documentation*, ANSYS, Inc., (2003).